Published in final edited form as:
J Neurosci. 2013 February 27; 33(9): 4118–4127. doi:10.1523/JNEUROSCI.4187-12.2013.

Increased agonist affinity at the mu-opioid receptor induced by prolonged agonist exposure

William T. Birdsong[1], **Seksiri Arttamangkul**[1], **Mary J. Clark**[2], **Kejun Cheng**[3], **Kenner C. Rice**[3], **John R. Traynor**[2], and **John T. Williams**[1]

[1]Vollum Institute, Oregon Health & Science University, Portland, OR, USA 97239

[2]Department of Pharmacology, University of Michigan, Ann Arbor, MI, USA 48109

[3]Chemical Biology Research Branch, National Institute on Drug Abuse and the National Institute on Alcohol Abuse and Alcoholism, NIH, Bethesda, MD, USA 20892

Abstract

Prolonged exposure to high-efficacy agonists results in desensitization of the mu opioid receptor (MOR). Desensitized receptors are thought to be unable to couple to G-proteins, preventing downstream signaling, however the changes to the receptor itself are not well characterized. In the current study, confocal imaging was used to determine whether desensitizing conditions cause a change in agonist-receptor interactions. Using rapid solution exchange, the binding kinetics of fluorescently labeled opioid agonist, dermorphin Alexa594 (derm A594), to MORs was measured in live cells. The affinity of derm A594 binding increased following prolonged treatment of cells with multiple agonists that are known to cause receptor desensitization. In contrast, binding of a fluorescent antagonist, naltrexamine Alexa 594, was unaffected by similar agonist pre-treatment. The increased affinity of derm A594 for the receptor was long-lived and partially reversed after a 45 min wash. Treatment of the cells with pertussis toxin did not alter the increase in affinity of the derm A594 for MOR. Likewise the affinity of derm A594 for MORs expressed in mouse embryonic fibroblasts derived from arrestin 1 and 2 knockout animals increased following treatment of the cells with the desensitization protocol. Thus, opioid receptors were “imprinted” with a memory of prior agonist exposure that was independent of G-protein activation or arrestin binding that altered subsequent agonist-receptor interactions. The increased affinity suggests that acute desensitization results in a long lasting but reversible conformational change in the receptor.

Introduction

Opioid agonists are widely used for the management of pain. The development of tolerance is a major clinical limitation in treating persistent pain in that effective pain relief often requires increasing doses of opioids. Activation of the mu opioid receptor (MOR) by highly efficacious agonists for as little as 5 minutes results in a decrease in downstream signaling, characterized as homologous receptor desensitization (Harris and Williams, 1991). Acute receptor desensitization may be the first step in a process leading to the development of tolerance.

Previous studies of receptor desensitization have focused on changes in signaling of downstream effectors to make inferences about changes in the receptor itself. Due to second

Corresponding author: John T. Williams, Vollum Institute, Oregon Health & Science University, 3181 SW Sam Jackson Park Rd, Portland OR 97239, USA, williamj@ohsu.edu.

Conflict of Interest: The authors declare no competing financial interests.

messenger signal amplification and variability in receptor-effector coupling, it is not clear how receptor desensitization relates to decline in effector readout. A large receptor reserve or efficient receptor-effector coupling can limit the downstream measurement of receptor desensitization. That is, a significant number of receptors can be desensitized while having little effect on effector activity if an efficacious agonist is used at high concentration (Connor et al., 2004). This has resulted in conflicting information about the role of various signaling pathways involved in mediating desensitization. Furthermore, investigations of acute desensitization have used various effectors in many different systems, which has created conflicting information and ideas about the processes governing desensitization (Chuang et al., 1998; Bohn et al., 2000; Tan et al., 2003; Schulz et al., 2004; Bailey et al., 2009; Dang et al., 2009; Arttamangkul et al., 2012).

The current model of desensitization, based on studies of the β2-adrenergic receptor, asserts that agonist binding and G-protein activation induces downstream kinase activation and phosphorylation by G-protein coupled receptor kinase (GRK). This phosphorylation leads to the recruitment of β-arrestin, which binds to receptors with high affinity preventing receptor association and activation of heterotrimeric G-proteins(Benovic et al., 1987; Dang and Christie, 2012). This model is assumed to hold true for MOR signaling though studies over the past 15 years have not convincingly elucidated a mechanism.

Real-time measurements of receptor-ligand interactions in living cells have the potential to examine desensitization at the level of the receptor itself without relying on changes in effector function. This study examines a receptor-based model of MOR desensitization in live cells. Fluorescent opioid ligands (an agonist and an antagonist) were imaged to study their binding kinetics to MOR in HEK293 cells that expressed a FLAG-tagged MOR. Prolonged treatment of MOR cells with a protocol known to result in desensitization dramatically slowed the rate of fluorescent agonist unbinding (dissociation) and increased affinity in a long-lived manner. Antagonist unbinding was unaffected. Thus, receptors were imprinted with a signature of previous exposure to agonists. The increase in affinity was agonist dependent but independent of G-protein signaling and β-arrestin proteins. These results suggest that conditions that are known to cause receptor desensitization also induced long-lived changes in agonist- receptor interactions that directly affected agonist affinity.

Methods

Materials

The following drugs were used in this study: [Met^5] enkephalin, oxycodone, concanavalin A, M1 anti FLAG, pertussis toxin, naloxone, β-chlornaltrexamine (Sigma Aldrich, St. Louis, MO) fentanyl, methadone, morphine (National Institute on Drug Abuse, Neuroscience), Alexa 488 SDP ester and Alexa 594 succinimidyl ester (Life Technologies, Grand Island, NY). M1 anti FLAG was conjugated with Alexa 488 SDP ester and purified using Bio-Spin 6 Tris columns (Bio Rad, Hercules, CA). Plasmids and stable cells lines for expression of FLAG tagged MOR were provided by Mark von Zastrow, Univ. of California San Francisco and pcDNA 3.1 plasmids encoding G-protein coupled inward rectifying potassium channels 1 and 2 (GIRK 1 and GIRK 2) were gifts from Kevin Wickman, Univ. of Minnesota.

Cell Culture

HEK 293 cells stably expressing FLAG tagged mu opioid receptor (FLAG-MOR) have been described previously (Keith et al., 1996). Cells were cultured in DMEM medium containing 10%FBS, 0.5% HEPES, 0.8% G418. Mouse embryonic fibroblast cells (MEF), created from wildtype or β arrestin 1/2 double knockout embryonic mice as described (Kohout et al., 2001), were a gift from Dr. Robert Lefkowitz, Duke University. MEF cells were efficiently

transfected using NeuroMag Magnetofection (OzBiosciences, Marseille, France) following manufacturer's protocol using 5 μg plasmid DNA and 8.5 μL NeuroMag solution per well of a 6 well dish.

Fluorescent Ligand Synthesis

Naltrexamine Alexa 594 (ntx A594) was synthesized as follows: The 6-beta-naltrexamine. 2HCl.0.75 H2O was synthesized as previously described (Sayre and Portoghese, 1980). The compound was dissolved in 0.1 M sodium bicarbonate and then reacted with Alexa 594 succinimidyl ester in DMSO with the molar ratio of 1:7. The crude product was purified by HPLC to at least 98% purity. The molecular mass of the product was further confirmed by electronspray ionization mass spectrometry by the Bioanalytic Shared Resource/ Pharmacokinetics Core, OHSU (BSR/PKCore).

The fluorescent peptide dermorphin Alexa 594 (derm A594) was synthesized as previously described (Arttamangkul et al., 2000). Briefly, the peptide (Tyr-D-Ala-Phe-Gly-Tyr-Pro-Lys-Cys-amide) was made using standard Fmoc solid phase peptide protocol. The crude peptide was purified by HPLC prior to conjugation with the Alexa 594 maleimide dye (Life Technologies). The final product was further purified by HPLC and its molecular mass confirmed by electronspray ionization mass spectrometry (BSR/PKCore).

Radioligand binding

HEK293 cells stably expressing FLAG-MOR were grown to confluency and harvested for membrane preparation as previously described (Clark et al., 2003). Cell membranes were thawed, Dounce homogenized and incubated (5 μg/well) for 60 min at room temperature with 0.2 nM [^{3}H]diprenorphine and 0–10 μM dermorphin Alexa594 or 10 μM naloxone (for non-specific binding) in Tris buffer (50 mM Tris-HCl, pH 7.4) or G buffer (50 mM Tris-HCl, pH 7.4, 100 mM NaCl, 5 mM $MgCl_2$, and 10 μM GTPγS). Samples were filtered through glass-fiber filter mats (Whatman, GF/C) using a Brandel cell harvester and rinsed three times with ice-cold Tris or G buffer. Filters mats were dried, scintillation cocktail (EcoLume, ICN, Aurora, OH) was added, and the filter mats were sealed in a polyethylene bag. Radioactivity retained on the filters was counted in a Wallac 1450 Microbeta liquid scintillation counter. Data were fit to a one or two site competition binding curve using GraphPad Prism to determine Ki. After determining that a one-site model better fit the data, the Hill slope was fixed to n= 1 to calculate the best fit.

Whole cell [^{3}H] DAMGO binding

FLAG-MOR expressing HEK293 cells grown in 24 well plates were pretreated by replacing the cell media with Krebs buffer containing 600 μg/ml concanavalin A and with or without 30 μM ME. After 2 h at 37°C, treatment buffer was replaced 2 times with Krebs buffer alone at 37°C, then with Krebs buffer containing 12 nM [^{3}H] DAMGO with or without 10 μM naloxone. The binding was stopped after 10 min at 37°C by putting the plate on ice and quickly replacing the assay buffer 2 times with ice cold Krebs buffer followed by replacement with cold 3% perchloric acid (or lysis buffer for protein samples). After 30 min on ice, samples were transferred to vials for liquid scintillation counting.

Imaging solution

Coverslips were perfused with Krebs buffer containing (in mM) NaCl 126, KCl 2.5, $MgCl_2$ 1.2 $CaCl_2$ 2.4, NaH_2PO_4 1.2, $NaHCO_3$ 21.4, glucose 11.1 and aerated with 5%CO_2/ 95% O_2. For fast solution exchange, $NaHCO_3$ and glucose were omitted and HEPES 15 was added, the pH adjusted to 7.4 with HCl, and osmolarity adjusted to 305 mOsm.

Imaging

Imaging was carried out on an Olympus BX51WI inverted microscope and Olympus LUMPlanFL N 60×/1.00 W objective. A Nipkow spinning disk confocal scanner (Solamere Technology) and ICCD camera (XR/MEGA 10, Stanford Photonics) were used to acquire rapid confocal images in a single plane using Piper data acquisition software (Piper Control 2.4.51, Stanford Photonics). Alexa 488 was imaged using a 488nm Argon ion laser (National Laser Company) while Alexa 594 was excited using a 561nm solid state laser (Cobolt Jive 25). Rapid switching between 488nm and 561nm was achieved via AOTF (NEOS). A quadruple band pass dichroic mirror (Di01 T403/488/568/647, Semrock) and dual bandpass emission filter (FF01-523/610, Semrock) were used.

Data Acquisition

FLAG tagged MOR was labeled with M1 anti-FLAG antibody conjugated to Alexa488 to allow for visualization of receptors on the plasma membrane. Solution exchange was achieved using computer controlled solenoid valves (Warner Instruments) to switch between two solutions that flowed through double barrel theta glass attached to a piezo bimorph (Piezo Systems) to facilitate exchange. Ratiometric imaging was carried out by taking serial images alternating between 488nm and 561nm excitation wavelengths to image Alexa488 and Alexa 594 respectively. A pair of images (100ms exposure each) was generally taken every 2.5 seconds before, during and after application of derm A594 to image baseline fluorescence, binding and unbinding respectively.

Steady state binding

Cells labeled with M1 A488 were incubated in various concentrations of derm A594 (3– 300 nM) and allowed to equilibrate for 5–10 min and subsequently imaged over 10– 15 minutes. Since there was no relationship between equilibration time and the amount of derm A594 bound, it can be concluded that derm A594 was largely equilibrated within 5 minutes (10nM derm A594 post ME treatment linear regression of incubation time vs. R/G value; $r=0.292$, $p=0.45$). A 5 sec puff of derm A594-free solution was applied during image acquisition to reduce background fluorescence. The images used for quantification were taken within 1 sec of derm A594 removal so that unbinding of derm A594 was minimal. Intensity of derm A594 binding relative to M1 488 (R/G) was measured and averaged for each concentration. To allow a direct comparison of binding under different conditions, measurement of steady state binding in untreated and ME treated cells was interleaved using the same stock solution of M1 A488 antibody to label surface receptors and the same derm A594 to assess binding.

Analysis

Image quantification was carried out using Image J software (Image J, NIH, Bethesda, MD) and the “Time Series Analyzer” plugin (Balaji J., Dept. of Neurobiology, UCLA). Analysis was done using Excel and Origin Lab software. Five background regions of interest (ROI) surrounding the cell of interest and one signal ROI encompassing the plasma membrane with as little intracellular area as possible were selected and the fluorescence intensity of each region was measured for each image frame in a time series for both 488nm and 561nm excitation wavelengths to measure M1 A488 anti-FLAG and derm A594 intensity respectively. The average of the 5 background ROI intensities was subtracted from the signal ROI for each frame and the ratio of derm A594: M1 A488 intensity was measured to give an R/G value. The magnitude of the R/G values are dependent upon efficiency of antibody- fluorophore conjugation, exposure time, laser intensity and efficiency of light collection for each wavelength and do not represent an absolute ratio of ligand bound per receptor. The average R/G value before exposure to derm A594 was taken to represent the baseline fluorescent signal in the absence of any derm A594. This baseline fluorescence was

subtracted from all R/G values in the time series. To compare the timecourse of binding and unbinding between experiments, the R/G intensities were normalized to the intensity of the first image after washout of derm A594 (unbinding) or the final image of derm A594 application (binding). The average fluorescence intensity of the signal ROI was generally about 5 times that of the background ROIs when measuring M1 A488 fluorescence. Derm A594 fluorescence signal was about 2 times above background when measuring unbinding, but only 5–10% above background ROI intensity when measuring binding at higher derm A594 concentrations.

For steady state ligand binding and competition assays, relative fluorescence intensity was plotted and fit using the Hill equation with a variable slope. For kinetic binding experiments, apparent association rate or dissociation rates were calculated by fitting data from each experiment with a single exponential decay function. All fitting was done using Origin Lab. Apparent association and unbinding rates were averaged among experiments. Apparent association of derm A594 (K_{obs}) as a function of concentration was plotted and linearly fit (Eq 1) according to a first order binding mechanism so that:

$$k_{obs}=k_{off}+k_{on}*[\mathrm{dermA594}] \quad \text{(Eq 1)}$$

with K_{on} being the slope of the line and K_{off} being the y-intercept and Kd calculated from

$$K_d=\frac{k_{off}}{k_{on}} \quad \text{(Eq 2).}$$

For ntx A594 binding, apparent association (k_{obs}) and unbinding rates (k_{off}) were measured using 100nM ntx A594 and Eq 1 was used to calculate the rate of association (k_{on}) and Eq 2 used to estimate K_d.

Results

Specificity of binding and unbinding of dermorphin Alexa 594 to mu opioid receptors

The fluorescent opioid agonist dermorphin-Alexa 594 (derm A594) was rapidly applied to HEK 293 cells stably expressing FLAG-tagged MOR to address whether derm A594 could be used to assay opioid receptor binding kinetics (Figure 1). Plasma membrane-localized FLAG-MOR receptors were labeled with the M1 anti-FLAG antibody conjugated to Alexa 488 (M1-A488) (Figure 1a). Binding and unbinding (dissociation) of derm A594 (100 nM, 90 sec) was imaged using a spinning disk confocal microscope. By measuring the fluorescence intensity of both derm A594 (red, R) and M1 488 (green, G) bound to the cell membrane, ratiometric quantification (R/G) of derm A594 binding relative to the receptor density was monitored (Fig 1b). Specificity of binding was confirmed by pre-incubating cells with the irreversible antagonist, β-CNA (1 μM, 5 min) and subsequently applying derm A594 (500 nM, 5 min) in the presence of the opioid antagonist naloxone (10 μM, Fig 1c). A high concentration of naloxone was used to increase the rate of naloxone binding to receptors since dermorphin A594 (500 nM) has a relatively fast apparent rate of association at this concentration. There was no appreciable fluorescence after β-CNA/naloxone treatment. Thus, derm A594 binds specifically to FLAG-MOR receptors in HEK293 cells and the kinetics of binding can be easily monitored.

MOR was largely in low affinity state in live cells

Agonist binding to MOR in membrane homogenates displays two affinity states, a high agonist affinity state thought to comprise a ternary complex between agonist, MOR and G-protein, and a low agonist affinity state believed to form between agonist and non-G-protein coupled MOR (Werling et al., 1988). Radioligand competition binding assays were carried

out to assess the ability of derm A594 to displace [^{3}H]-diprenorphine bound to membrane homogenates from HEK 293 cells stably expressing FLAG-MOR. Displacement assays were performed in 50 mM TRIS to observe high affinity binding and 50 mM TRIS in the presence of Na^+, Mg^{2+} and GTPγS to displace G-proteins and observe low affinity binding. Derm A594 displaced [^{3}H]-diprenorphine with a K_i of 2.9±0.8 nM in TRIS and 120±40 nM in TRIS plus Na^+, Mg^{2+} and GTPγS (Fig 2a, avg. of 3 experiments in duplicate, Table 1) revealing high and low affinity agonist binding. Under both conditions the data were best fit to a one site model. The large shift in affinity upon addition of Na^+, Mg^{2+} and GTPγS is indicative of an agonist with generally high efficacy (Lee et al., 1999).

Next, binding of derm A594 was characterized in live HEK293 cells stably expressing FLAG-MOR to determine whether binding in live cells resembled high or low affinity binding seen in the displacement assay. Cells were maintained in HEPES buffered modified KREB's solution to mimic physiological ionic conditions as much as possible. M1 A488 was used to visualize surface-localized receptors. Derm A594 (3 nM – 300 nM) was added to the bath solution, allowed to equilibrate at room temperature and the ratio of derm A594 bound to cells relative to M1 488 was measured. Half maximal "steady state" binding was estimated to be approximately 85 nM derm A594 determined by the best fit of the data (EC_{50} = 85 nM, 50 – 142 nM 95% CI, Hill slope=0.95±.02, Figure 2b, n= 5–11 cells for each concentration). This more closely resembled the low agonist affinity binding rather than high agonist affinity binding observed in typical binding assays performed in the absence of sodium. No saturation of whole cell binding could be observed since derm A594 (300 nM) was the highest concentration possible to image before background fluorescence became unacceptable. Thus, it is possible that the observed binding affinity could appear artificially high and the actual value may be closer to the 120 nM low affinity state. It should be noted that the R/G values in figure 2b are dependent upon the exposure time for each image, relative laser intensity, efficiency of fluorescence excitation and collection of emitted light. Thus, the maximum R/G value of 4 does not represent an absolute ratio of 4 derm A594 molecules bound per FLAG epitope and the absolute ratio was not determined in these assays.

Binding kinetics was also used to assess the interaction between derm A594 and MOR in live cells at room temperature. Derm A594 was rapidly applied at 10, 30, 100, and 200 nM (Fig 2c, n=4–7) and the apparent rate of association was measured. The apparent on rate was plotted as a function of derm A594 concentration (Figure 2d) and fit linearly according to equation 1 to yield an association rate of 612,000±114,000 $(mol*sec)^{-1}$, a rate of dissociation of 0.068± 0.006 sec^{-1} and a calculated K_d of approximately 111 nM (85– 149 nM range, Equation 2). Thus, using non- equilibrium binding kinetics, the calculated affinity of derm A594 for MOR was similar to live cell steady state measurements and radioligand competition results from membrane homogenates in the presence of sodium and GTPγS.

Pertussis toxin is known to eliminate activation of $G_{i/o}$ G-proteins by MOR and to reduce high affinity binding of agonists to MOR in the presence of sodium (Kurose et al., 1983; Wüster et al., 1984). If high affinity binding, which is sodium and G-protein dependent, makes a significant contribution toward the interaction of agonist and receptor in live cells, one would expect pertussis treatment to decrease the affinity and alter the kinetics of agonist binding to MOR receptor. Treatment with pertussis toxin, however, had no effect on the kinetics of derm A594 binding and unbinding (Figure 2e). Pertussis toxin treatment did block the activation of GIRK current by ME (1 μM, 5 sec) in cells transiently co-expressing FLAG-MOR, GIRK1 and GIRK2 (untreated: 171±61 pA n=5; pertussis toxin 100 ng/mL overnight: 3.3±6.8 pA n=4) confirming its effectiveness at disrupting $G_{i/o}$ signaling. This suggests that, while the high affinity state is likely important for activation of G-proteins and subsequent signaling, most binding and unbinding events in live cells occurred to/from the

low affinity state. Taken together these results suggest that binding of derm A594 to receptors in live cells under physiological conditions most closely resembles low affinity binding seen in traditional radioligand binding assays being both relatively low affinity and pertussis toxin insensitive. This is consistent with many previous observations that sodium and GTP – present at high concentrations under physiological conditions - lower the affinity of many agonists for GPCRs.

Desensitizing conditions induced a persistent change in agonist-receptor interaction

Classically, desensitization has been defined by a decrease in receptor mediated signaling in response to prolonged application of high concentrations of efficacious agonists. Full agonists such as the endogenous opioid agonist [Met^5] enkephalin (ME) cause robust desensitization while partial agonists such as morphine are less effective (Dang and Williams, 2005). If the process of desensitization results in a change in receptor conformation state rather than simply a loss of downstream signaling, the kinetics of ligand-receptor interactions may be predicted to change. Therefore, the rate of derm A594 unbinding was used as a reporter for changes in MOR conformation in response to desensitizing agonist exposure. FLAG-MOR expressing cells were incubated at 37°C and either untreated, or treated for 2 min, 20 min or 2 hrs in ME 30 μM (a desensitizing concentration) in the presence of concanavalin A (ConA, 200–600 μg/ml) to reduce MOR internalization. After ME treatment, cells were washed for one minute and transferred to an imaging chamber during which time cells were perfused with room temperature Kreb's buffer. After 5 minutes in the imaging chamber, binding and unbinding was measured by imaging FLAG-MOR cells while a 60 or 90 sec application of derm A594 (100 nM) was applied. The experimental outline is diagrammed at the top of figure 3. Surprisingly, pretreatment with ME dramatically slowed the rate of subsequent unbinding of derm A594 (Fig 3A). The slowed rate of unbinding was quantified by determining the fraction of dermA594 remaining 3 min after washout. The fraction of derm A594 that remained bound after 3 min increased dramatically (Fig. 3B; fraction remaining; untreated, 0.16±0.01, n=9; ME 30 μM, 2 min, 0.25± 0.03 n=6; ME 30 μM, 20 min, 0.39±0.02 n=11; ME 30 μM 2 hr, 0.52±0.02, n=7). Thus, although ME was washed from the receptors, MOR pretreated with ME maintained a persistent signature of prior agonist exposure that resulted in a change in the kinetics of subsequent binding of derm A594 to the receptor.

Demonstrating a concentration dependence, a sub-saturating concentration of ME (300 nM) applied for 20 min induced a modest change in derm A594 unbinding rate similar to that induced by 2 min of ME 30 μM (fraction derm A594 remaining= 0.27± 0.02, n=4, data not shown). Receptor modulation by agonist exposure persisted after ME washout. Cells that were washed for 45 min at 37°C after a 1 hr exposure to ME showed approximately 65% reversal of the change in derm A594 unbinding rate (fraction derm A594 remaining: 1 hr ME, 0.45±0.01 n=6; 1 hr ME/45 min wash, 0.26±0.01 n=7, untreated, 0.16±0.01, n=9 data not shown). Taken together, there was a change in the kinetics of derm A594 unbinding that was dependent upon both time and concentration of ME pre-exposure, which reversed slowly over tens of minutes.

Agonist treatment increased agonist affinity

If the rate of unbinding of dermA594 slowed with little or no change in the rate of association, the affinity of the agonist for the receptor should increase. Steady state binding in live cells was used to estimate the affinity of derm A594 for FLAG MOR after preincubation of cells with ME (30 μM 2 hr, Figure 3c). After ME treatment, the cells were washed, various concentrations of derm A594 were applied and the amount of derm A594 bound relative to M1 A488 intensity was measured and plotted (Figure 3c, red). The steady state binding curve shown in figure 2b measured under naïve conditions is overlaid for

reference (black). After pretreatment with ME, there was a leftward shift of the derm A594 binding curve (n=7–19 cells for each concentration). The EC_{50} of the best fit of the data increased from approximately 85 nM to 12 nM (Table 1) after incubation in ME (30 μM, 2 hrs), indicating that desensitizing conditions increased the affinity of agonist for receptor. The Hill slope wash unchanged (1.03±0.3). Consistent with ME treatment increasing the affinity of MOR for derm A594, following ME treatment there was a large increase in derm A594 binding to MOR at low concentrations (derm A594, 10 nM, 275±87% increase following ME treatment) that was not seen at high concentrations (derm A594, 300 nM, 12±6% increase following ME treatment, Figure 3c). This observation suggests a leftward shift in the binding curve rather than a large change in the number of available binding sites and that 300 nM derm A594 is nearly saturating MOR binding sites.

The apparent association rate was also measured to assess whether prolonged ME treatment increased the affinity of derm A594 for MOR. As was done in untreated cells (figure 2c, d), the binding of derm A594 to cells preincubated with ME (30 μM 2 hr) was imaged using various concentrations of derm A594 (10–200 nM). Binding of derm A594 (30 nM) to untreated cells (black) and ME treated cells (red) revealed that the average time constant of association increased from 11.4±0.4 sec to 51.5±7.8 sec (Figure 3d, n=4 each). A plot of the apparent association rate as a function of derm A594 concentration (Figure 3e) was linearly fit in untreated cells (black, from figure 2d) and cells treated with ME (red). After ME treatment, k_{on} decreased by about 40% to 353,000±29,000 M^{-1} sec^{-1} while k_{off} decreased approximately 6 fold to 0.011±0.002 sec^{-1} yielding a calculated K_d of 32 nM (24–42 nM range). Thus, prolonged exposure of live FLAG-MOR expressing cells to ME caused an increase in the subsequent affinity of derm A594 for MOR measured using both steady state and kinetic assays. Since prolonged exposure to ME both slowed the rate of unbinding and increased the affinity of MOR for derm A594, unbinding rate will be used as a proxy for affinity measurements throughout this manuscript.

Increased affinity of non-fluorescent opioid agonists

Two different assays were performed to determine whether an increase in binding affinity after prolonged ME treatment was common to other agonists. First, a sub-saturating concentration of [^{3}H] DAMGO (12 nM, 10 min) was applied to live FLAG-MOR HEK 293 cells that were naïve or pretreated with ME (30 μM, 2 hrs, + Con A 600 μg/ mL) and the amount of specifically bound [^{3}H] DAMGO was quantified. Consistent with steady state binding of derm A594 (10 nM) shown in figure 3c, there was a 335% increase in [^{3}H] DAMGO binding after modulation by ME (naïve, 91.3±2.3; ME 2 hrs, 397.7± 32.6 fmol [^{3}H] DAMGO bound/mg protein, n=3, data not shown). The large increase in binding at sub-saturating agonist concentrations is consistent with DAMGO behaving in a similar fashion to derm A594, showing increased affinity for receptors that were previously modulated by ME.

Second, the unbinding rate of ME was inferred from its ability to slow the apparent rate and extent of derm A594 binding. The binding of derm A594 will be occluded as long as ME remains bound to receptors. The pulse-chase like assay diagrammed in Figure 4a used a prepulse of ME (3μM, 1min) instead of buffer immediately preceding application of dermA594 to test whether ME unbinding was slowed after prolonged ME exposure. After prolonged ME treatment (30 μM, 2hrs) and wash, followed by either buffer or ME-prepulse (3 μM, 1min), derm A594 (200nM, 1 min) was applied and the relative amount of derm A594 bound was measured. Cells subjected to ME-prepulse (3 μM, 1min) bound approximately 1/3 less dermA594 than cells washed with buffer solution (Figure4a-i, ME 30 μM, 2 hrs; then buffer R/G= 1.44±0.10, or ME 3 μM pre pulse R/G= 0.95±0.08, n=6 each)). There was no difference in the amount of derm A594 bound after 1 minute when naïve cells were pre pulsed with either ME (3 μM, 1 min) or buffer (Figure 4a-i, untreated; then buffer

R/G= 0.84±0.07, or ME 3 μM pre pulse R/G= 0.88±0.07, n=5 each) suggesting that ME rapidly and completely unbound from MOR in naïve cells.

Binding of derm A594 to untreated cells immediately following a 1 minute pre-pulse of ME (3 μM, 1 min) occurred with an apparent time constant of association of 8.5± 0.3 sec, only slightly slower than the tau of 5.6± 0.2 sec observed when there was no ME prepulse (Figure 4a-ii, n=6 each). This indicates that under naïve conditions, ME rapidly dissociated from the receptor allowing derm A594 to bind. After the prolonged ME treatment (30 μM 2 hrs), the basal rate of association of derm A594 slowed down (τ=12.3± 0.1 sec) and the ME prepulse further slowed the apparent association (τ=26.6± 2.9 sec) (Figure 4a-iii, n=7 each) suggesting that ME unbound from the receptor more slowly after the receptor had been desensitized with prolonged ME. Thus after treatment with ME (30 μM, 2 hrs), the rate of unbinding of an unlabeled endogenous peptide, ME, was slowed as was derm A594 suggesting that ME affinity increased following extended ME treatment.

In figure 4a it was demonstrated that ME could remain bound for an extended period to some receptors that were pretreated with ME (30 μM 2 hrs). To determine whether this remaining ME had an effect of derm A594 kinetics, the unbinding of derm A594 was measured. Cells were pre-incubated with ME for a shorter period of time (30 μM, 20 min) to allow determination of whether an ME prepulse increased, decreased or had no effect on the rate of subsequent derm A594 unbinding. When ME (3 μM) was applied both before (1 min pulse) and after application of derm A594 to cells previously treated with ME (30 μM, 20 min), the rate of derm A594 unbinding was increased relative to cells that were rinsed with buffer (Figure 4b-ii). After a 1 min exposure to ME (1 μM), the fraction of derm A594 remaining after 3 min was not significantly different from untreated cells (Figure 4b-i, fraction remaining: untreated 0.15±0.01 n=9, ME /ME/ ME 0.20±0.03, n=7). One interpretation of this result is that there were two populations of receptors following incubation with ME (30 μM). One population, having a slow unbinding rate, remained bound to ME preventing the binding of derm A594. In the second population, ME quickly dissociated allowing derm A594 to bind. Thus derm A594 bound only to the rapidly dissociating population of receptors such that derm A594 also dissociated rapidly.

Affinity changes independent of solution exchange

An alternative explanation for the relative speeding of derm A594 unbinding is that ME present during derm A594 washout displaced derm A594 through bulk displacement or negative cooperativity. ME treated cells (30 μM, 20 min) were washed with buffer, exposed to derm A594, and then washed with either buffer “infinite dilution” (ME/ buffer/ buffer, open squares, figure 4b-ii) or ME (3 μM) “displacement” (ME/ buffer/ ME, blue) to address these possibilities. Displacing derm A594 with ME had no effect on the rate of unbinding (fraction derm A594 remaining: ME/ dilution 0.39±0.02 n=11, ME/ displace 0.37±0.2 n=7, Figure 4b-i) suggesting that rapid agonist rebinding, cooperative binding, or poor solution exchange were insufficient to explain the observed change in agonist affinity induced by prior ME exposure (DeMeyts et al., 1976; Spivak et al., 2006).

Ligand dependence of derm A594 affinity change

FLAG-MOR expressing cells were next pretreated with a series of opioid ligands including agonists ME (30 μM), methadone (15 μM), endomorphin 2 (30 μM), fentanyl, morphine and oxycodone or the antagonist naloxone (10 μM unless noted otherwise, 2 hr) to determine ligand specificity of agonist modulation (Figure 5b). Slowed unbinding was quantified by determining the fraction of derm A594 bound to MOR 3 min after washout (Figure 5a, c). Consistent with the efficacy and desensitization profile of each ligand (Virk and Williams, 2008; Rivero et al., 2012), ME, fentanyl, endomorphin 2, and methadone, all efficacious and

desensitizing agonists induced robust changes in the rate of unbinding (fraction derm A594 remaining after 3 min: untreated: 0.15±0.01, ME: 0.52±0.02, fentanyl: 0.57±0.01, enodmorphin 2: 0.45±0.02, methadone: 0.44±0.01, n=5–9). Morphine pretreatment resulted in a partial change in unbinding rate relative to ME. Oxycodone pretreatment, which causes even less desensitization than morphine, resulted in less derm A594 remaining after 3 min (morphine: 0.29±0.03 n=7, oxycodone: 0.23±0.01 n=6). Pretreatment with naloxone had no significant effect on the fraction of derm A594 bound after 3 min (0.12±0.01, n=6). In summary, ligand induced modulation of agonist-receptor interaction was dependent upon both ligand relative efficacy (with the exception of endomorphin 2) and the duration of ligand exposure and correlated with the ability of agonists to induce desensitization.

Antagonist binding not changed

A novel fluorescent antagonist naltrexamine-Alexa594 (ntx A594) was synthesized and found to bind specifically to MOR in a manner that was inhibited by binding of the irreversible antagonist β-CNA (Fig 6b). The rate of dissociation (tau= 184±6.1 sec) and apparent rate of association (65.8±5.5 sec) of ntx A594 (100 nM, Figure 6a) yielded estimated Kd of 53 nM. In contrast to derm A594, the rate of unbinding of ntx A594 was unaffected by pretreatment of FLAG-MOR cells with ME (30 μM, 2 hr, Figure 6c). Taken together, the results demonstrate that ME exposure can induce a change in affinity of agonist but not antagonist labeled with the identical fluorophore, suggesting that modulation is specific to agonists.

Role of G-proteins and β-arrestins

Several possible mechanisms could account for the long-lasting memory of prior agonist exposure. Since the effect of agonist pretreatment persisted long after washout of agonist, GPCR signaling pathways were considered. MOR classically signals through inhibitory G-proteins and non-classically through β-arrestin. Cells that were treated overnight with pertussis toxin, eliminating inhibitory G-protein signaling, still showed a robust slowing in derm 594 unbinding following treatment with ME (30 μM, 2 hr, Figure 7a, fraction remaining: Untreated, ctrl= 0.15±0.01, ptx= 0.13±0.005; ME 2 hrs, ctrl= 0.54±0.02, ptx= 0.51±0.01, n= 3–5, figure 7b). This suggested that G-protein signaling and $G_{i/o}$ mediated GRK phosphorylation were not responsible for this modulation.

To address the possible role of arrestins in agonist induced imprinting, β-arrestin 1 and 2 double knockout MEF (β-arr 1/2 k.o.) cells and wildtype (WT) controls were transiently transfected with FLAG-MOR and the unbinding of derm A594 was measured. Loss of both β-arrestin 1 and 2 had no effect on the ability of agonist to induce a slowing in the rate of unbinding (Figure 7c). The rate and extent of unbinding was nearly identical between WT and β-arr 1/2 k.o. MEF cells both before and after treatment with ME (30 μM, 2 hrs) (fraction remaining after 3 min: untreated, WT=0.09±0.01, β-arr k.o.= 0.13±0.02; ME 2 hr, WT= 0.50±0.05, β-arr k.o.=0.47±0.04, n=5, Figure 7d). Finally, pertussis toxin treatment of β-arr 1/2 k.o. MEF cells had no effect on the ability of ME treatment to modulate derm A594 affinity indicating that there are not parallel pathways of modulation involving both G-protein signaling and arrestin signaling (fraction remaining after 3 min: untreated= 0.12±0.02, ME 30 μM, 2 hrs= 0.51±0.01 n=4 each, Figure 7d).

Discussion

Experiments measuring binding of opioids to receptors on live cells are not often performed, yet they have the potential to better our understanding of opioid pharmacology at the level of binding and the functional effects of opioids on MOR mediated signaling at the cellular level. One aim of this study was to gain insight into basic features of opioid ligand-receptor

interactions in live cells. This was pursued with the goal of determining whether desensitization, which has been defined at the cell signaling level, could also be defined at the receptor level. The results presented here suggest that conditions that are known to desensitize receptors at the functional level also modulate receptor-agonist but not receptor-antagonist interactions suggesting a long-lived change in receptor conformation states that affect agonist binding and unbinding kinetics. Furthermore this agonist-induced change in affinity is independent of G-protein and β-arrestin signaling.

The increase in affinity and slowed binding and unbinding kinetics demonstrated here after prolonged ME treatment occurred in receptors that were desensitized. It has not, however, been determined whether the increase in agonist affinity, indicating a distinct conformation state, and acute desensitization of signaling are one and the same, rather that there is a correlation between desensitizing agonist exposure and agonist- receptor affinity changes. Both phenomena share a similar agonist profile and recover over a similar timescale (Virk and Williams, 2008; Rivero et al., 2012). While acute desensitization can be induced in as little as 1–2 minutes (Johnson et al., 2006), the change in agonist affinity occurs over a generally longer timescale, though this timescale is in line with other measures of cellular desensitization in HEK 293 cells (Koch et al., 1998). It is possible that multiple desensitized states of the receptor exist over different time scales. Thus, it is difficult to directly compare the current results based on direct receptor measurements with previous observations based on downstream signaling.

Receptor desensitization results in a decline in signaling due to a functional uncoupling of receptors and G-protein subunits. While this decline in signaling can be dramatic, prolonged exposure to agonist can never completely abolish signaling, suggesting that there are always some functional receptors present. After two hours of exposure to ME, fentanyl, endomorphin 2, or methadone, derm A594 unbinding was dramatically slowed. Mirroring functional studies suggesting that both desensitized and functional receptors are always present, the unbinding of derm A594 after agonist imprinting was always poorly fit with a single exponential and was better fit with both a fast and slow unbinding component. Since cells that are not pre-exposed to desensitizing agonist show predominantly fast unbinding, it is proposed that the fast unbinding receptors are functional and the slow unbinding receptors are desensitized.

The canonical model of GPCR desensitization involves binding of β-arrestin to phosphorylated receptors. The binding of β-arrestin is proposed to prevent binding of the G-protein to the receptor, disrupting signaling (Benovic et al., 1987, Luttrell and Lefkowitz, 2002). High affinity binding of agonists to GPCRs is thought to be mediated by intimate association of the heterotrimeric G-protein with the opioid receptor (Da Lean et al., 1980). Loss of coupling between receptor and G-protein through desensitization would be expected to result in a loss of high affinity binding and thus a decrease in affinity. However, our results suggest that the opposite occurred in live cells where the affinity was increased after exposure to desensitizing agonists. While many ligand gated ion channels, such as the nicotinic acetylcholine receptor (Heidmann et al., 1983), display increased agonist affinity when in a desensitized state, this has not been reported for G-protein coupled receptors.

The mechanism for the prolonged agonist binding must differ from that of ligand gated ion channel desensitization whereby desensitized receptors remain bound to agonist while desensitized and upon unbinding of agonist, desensitization is reversed. Since derm A594 binding and unbinding are affected by prior agonist exposure, it is clear that MOR has retained a “memory” of desensitization that persisted after the agonist was removed. Receptor phosphorylation is one mechanism by which information about prior agonist-induced conformational changes could be encoded into a persistent change at the receptor

level and many functional studies of MOR desensitization implicate a role of kinases in the processes of desensitization and recovery from desensitization (Bailey et al., 2009; Dang et al., 2009; Arttamangkul et al., 2012; Dang and Christie, 2012). It has recently been demonstrated that receptor phosphorylation in the C-terminal tail is induced in a ligand dependent manner similar to agonist treatments described here (Doll et al., 2011; Lau et al., 2011). While it is recognized that agonists can induce phosphorylation of MOR, it is generally assumed that phosphorylation mechanisms involve downstream signaling for recruitment of kinases to the active receptor, though not all GRKs require G-proteins for recruitment to GPCRs. Additionally, tyrosine residues in the intracellular loops and C-terminal tail of MOR undergo phosphorylation in a manner that may be agonist-dependent but G-protein-independent (Pak et al. 1999, McLaughlin and Chavkin 2001). The present results suggest that neither G-protein nor β-arrestin mediated signaling were required for agonist modulation of MOR to alter subsequent agonist affinity and future studies will address whether phosphorylation is involved.

Multiple conformational states are known to exist in MOR and other GPCRs. Opioid receptor dissociation kinetics can be modulated by both sodium and GTP indicating the existence of multiple conformational states (Kurowski et al., 1982). The unbinding kinetics of peptide agonists from both MOR and DOR have been previously reported to be dependent on the time of agonist incubation using radioligand binding assays from hippocampal synaptic membranes, though this time dependent slowing in unbinding rate was eliminated by the presence of sodium perhaps suggesting an involvement of G-proteins and stabilization of the ternary complex (Scheibe et al., 1984).

Recent studies have found evidence for dynamic changes in conformation and affinity of other GPCRs. Purified, solubilized β2-adrenergic receptors undergo a fast conformation change upon initial binding of agonists and then a slow conformation change in the continued presence of some but not all agonists (Swaminath et al., 2004). NK2 receptors in intact cells display a time dependent change in the rate of fluorescent ligand unbinding with a desensitizing fluorescent peptide but not a shorter, non-desensitizing peptide (Palanche et al., 2001). Both of these studies have noted the relationship between these slow changes and desensitizing agonists, but have not investigated further. Repetitive activation of the β2-adrenergic receptor by agonist altered the kinetics of subsequent activation, suggesting a transient memory of previous agonist exposure (Ahles et al., 2011). The current results further support and expand upon the existence and ligand modulation of multiple affinity states suggesting that several G-protein and β-arrestin independent conformational states exist for MOR which are agonist-sensitive yet antagonist-insensitive. Furthermore, this study demonstrates a long-lived modulation of affinity, in which imprinting lasted for tens of minutes after washout of agonist in live cells.

As had been long predicted, the low affinity binding state may be the most physiologically relevant state of opioid agonist-receptor interactions as judged by binding in live cells (Carroll et al., 1988). This was supported by two observations: 1) Derm A594 binding in whole cells had an affinity close to that of the low-affinity radioligand competition binding measured in the presence of Mg^{2+}, Na^{+} and GTPγS and 2) pertussis toxin had no effect on the kinetics of binding or unbinding of dermA594. It is also notable that while derm A594 has a relatively high affinity for MOR even in the low affinity state (120 nM), dissociation of derm A594 from the receptor was rapid with a time constant on the order of 10 sec. In live cells, rapid dissociation is a common property of most opioid agonists (Ingram et al., 1997) perhaps due to the relatively exposed binding pocket as noted in the recent x-ray crystallographic structure of MOR (Manglik et al., 2012).

In summary, a novel approach for studying opioid receptor dynamics has demonstrated that prolonged exposure to desensitizing agonists can be imprinted onto receptors. This study suggests that agonist modulation affects the subsequent conformational changes induced by agonists, increasing agonist affinity and stabilizing agonist binding. While a definitive link between functional agonist-induced desensitization of receptor mediated signaling and physical agonist-induced modulation of agonist affinity has not been established, both the agonist dependence and time course of action are similar (Virk and Williams, 2008; Rivero et al., 2012). Further, this technique could be adapted for live-cell screening applications such as screens for allosteric modulators of agonist binding. The ease of manipulation of this system will allow pharmacological and structure-function based investigation of the mechanism of agonist modulation and determination of how physical changes at the receptor level affect receptor function and signaling.

Acknowledgments

Supported by: NIH DA08136. JRT and MJC were supported by MH083754. The Intramural Research Programs of National Institute on Drug Abuse and National Institute on Alcohol Abuse and Alcoholism supported a portion of this work. We would like to thank Dr. Shane Hentges for feedback during manuscript preparation, Dr. Erica Levitt for manuscript feedback and Graphpad expertise, and Dr. Dale Fortin for technical assistance.

References

Ahles A, Rochais F, Frambach T, Bünemann M, Engelhardt S. A polymorphisms-pecific “memory” mechanism in the β(2)-adrenergic receptor. Sci signaling. 2011; 4:ra53.

Arttamangkul S, Alvarez-Maubecin V, Thomas G, Williams JT, Grandy DK. Binding and internalization of fluorescent opioid peptide conjugates in living cells. Mol Pharmacol. 2000; 58:1570–1580. [PubMed: 11093798]

Arttamangkul S, Lau EK, Lu H-W, Williams JT. Desensitization and trafficking of μ-opioid receptors in locus ceruleus neurons: modulation by kinases. Mol pharmacol. 2012; 81:348–355. [PubMed: 22113080]

Bailey CP, Llorente J, Gabra BH, Smith FL, Dewey WL, Kelly E, Henderson G. Role of protein kinase C and mu-opioid receptor (MOPr) desensitization in tolerance to morphine in rat locus coeruleus neurons. Euro J Neurosci. 2009; 29:307–318.

Benovic JL, Kühn H, Weyand I, Codina J, Caron MG, Lefkowitz RJ. Functional desensitization of the isolated beta-adrenergic receptor by the beta-adrenergic receptor kinase: potential role of an analog of the retinal protein arrestin (48-kDa protein). Proc Natl Acad Sci USA. 1987; 84:8879–8882. [PubMed: 2827157]

Bohn LM, Gainetdinov RR, Lin FT, Lefkowitz RJ, Caron MG. Mu-opioid receptor desensitization by beta-arrestin-2 determines morphine tolerance but not dependence. Nature. 2000; 408:720–723. [PubMed: 11130073]

Carroll JA, Shaw JS, Wickenden AD. The physiological relevance of low agonist affinity binding at opioid mu-receptors. Brit J Pharmacol. 1988; 94:625–631. [PubMed: 2840167]

Chuang HH, Yu M, Jan YN, Jan LY. Evidence that the nucleotide exchange and hydrolysis cycle of G proteins causes acute desensitization of G-protein gated inward rectifier K+ channels. Proc Natl Acad Sci USA. 1998; 95:11727–11732. [PubMed: 9751733]

Clark MJ, Harrison C, Zhong H, Neubig RR, Traynor JR. Endogenous RGS protein action modulates mu-opioid signaling through G alpha o. Effects on adenylyl cyclase, extracellular signal-regulated kinases, and intracellular calcium pathways. J Biol Chem. 2003; 278:9418–9425. [PubMed: 12524446]

Connor M, Osborne PB, Christie MJ. Mu-opioid receptor desensitization: is morphine different? Brit J Pharmacol. 2004; 143:685–696. [PubMed: 15504746]

Da Lean A, Stadel JM, Lefkowitz RJ. A ternary complex model explains the agonist-specific binding properties of the adenylate cyclase-coupled beta-adrenergic receptor. J Biol Chem. 1980; 255:7108–7117. [PubMed: 6248546]

Dang VC, Christie MJ. Mechanisms of rapid opioid receptor desensitization, resensitization and tolerance in brain neurons. Brit J Pharmacol. 2012; 165:1704–1716. [PubMed: 21564086]

Dang VC, Napier IA, Christie MJ. Two distinct mechanisms mediate acute mu-opioid receptor desensitization in native neurons. J Neurosci. 2009; 29(10):3322–3327. [PubMed: 19279269]

Dang VC, Williams JT. Morphine-Induced mu-Opioid Receptor Desensitization. Mol Pharmacol. 2005; 68:1127–1132. [PubMed: 16020743]

DeMeyts P, Bainco AR, Roth J. Site-site interactions among insulin receptors. Characterization of the negative cooperativity. J Biol Chem. 1976; 251:1877–1888. [PubMed: 5434]

Doll C, Konietzko J, Pöll F, Koch T, Höllt V, Schulz S. Agonist-selective patterns of μ-opioid receptor phosphorylation revealed by phosphosite-specific antibodies. Brit J Pharmacol. 2011; 164:298–307. [PubMed: 21449911]

Harris G, Williams JT. Transient homologous mu-opioid receptor desensitization in rat locus coeruleus neurons. J Neurosci. 1991; 11:2574–2581. [PubMed: 1651377]

Heidmann T, Bernhardt J, Neumann E, Changeux JP. Rapid kinetics of agonist binding and permeability response analyzed in parallel on acetylcholine receptor rich membranes from Torpedo marmorata. Biochemistry. 1983; 22:5452–5459. [PubMed: 6652072]

Ingram S, Wilding TJ, McCleskey EW, Williams JT. Efficacy and kinetics of opioid action on acutely dissociated neurons. Mol Pharmacol. 1997; 52:136–143. [PubMed: 9224823]

Johnson EA, Oldfield S, Braksator E, Bonzalez-Cuello A, Couch D, Hall KJ, Mundell SJ, Bailey CP, Kelly E, Henderson G. Agonist-selective mechanisms of mu-Opioid receptor desensitizaiton in human embryonic kidney 293 cells. Mol. Pharmacol. 2006; 70:676–685. [PubMed: 16682505]

Keith DE, Murray SR, Zaki P a, Chu PC, Lissin DV, Kang L, Evans CJ, von Zastrow M. Morphine activates opioid receptors without causing their rapid internalization. J Biol Chem. 1996; 271:19021–19024. [PubMed: 8702570]

Koch T, Schulz S, Schröder H, Wolf R, Raulf E, Höllt V. Carboxyl-terminal splicing of the rat mu opioid receptor modulates agonist-mediated internalization and receptor resensitization. J Biol Chem. 1998; 232:13652–13657. [PubMed: 9593704]

Kohout TA, Lin F-T, Perry SJ, Conner DA, Lefkowitz RJ. Beta-Arrestin 1 and 2 differentially regulate heptahelical receptor signaling and trafficking. Proc Natl Acad Sci USA. 2001; 98:1601–1606. [PubMed: 11171997]

Kurose H, Katada T, Amano T, Ui M. Specific uncoupling by islet-activating protein, pertussis toxin, of negative signal transduction via alpha-adrenergic, cholinergic, and opiate receptors in neuroblastoma x glioma hybrid cells. J Biol Chem. 1983; 258:4870–4875. [PubMed: 6300102]

Kurowski M, Rosenbaum JS, Perry DC, Sadi WE. [3H]-Etorphine and [3H]-Diprenorphine Receptor Binding In Vitro and In Vivo: Differential Effect of Na + and Guanylyl Imidodiphosphate. Brain Res. 1982; 249:345–352. [PubMed: 6291717]

Lau EK, Trester-Zedlitz M, Trinidad JC, Kotowski SJ, Krutchinsky AN, Burlingame AL, von Zastrow M. Quantitative encoding of the effect of a partial agonist on individual opioid receptors by multisite phosphorylation and threshold detection. Sci Signaling. 2011; 4:ra52.

Lee KO, Akil H, Woods JH, Traynor JR. Differential binding properties of oripavines at cloned mu- and delta-opioid receptors. Euro J Pharmacol. 1999; 378:323–330.

Luttrell LM, Lefkowitz RJ. The role of beta-arrestin in the termination and transduction of G-protein-coupled receptor signals. J Cell Sci. 2002; 115:455–465. [PubMed: 11861753]

Manglik A, Kruse AC, Kobilka TS, Thian FS, Mathiesen JM, Sunahara RK, Pardo L, Weis WI, Kobilka BK, Granier S. Crystal structure of the μ-opioid receptor bound to a morphinan antagonist. Nature. 2012; 485:321–326. [PubMed: 22437502]

McLaughlin JP, Chavkin C. Tyrosine phosphorylation at the mu-opioid receptor regulates agonist intrinsic efficacy. Mol Pharmacol. 2001; 59:1360–1368. [PubMed: 11353794]

Pak Y, O'Dowd BF, Wang JB, George SR. Agonist-induced, G protein-dependent and -independent down-regulation of the mu opioid receptor. J Biol Chem. 1999; 274:27610–27616. [PubMed: 10488100]

Palanche T, Ilien B, Zoffmann S, Reck M, Bucher B, Edelstein SJ, Galzi J. The Neurokinin A Receptor Activates Calcium and cAMP Responses through Distinct Conformational States *. Biochemistry. 2001; 276:34853–34861.

Rivero G, Llorente J, McPherson J, Cooke A, Mundell SJ, McArdle CA, Rosethorne EM, Charlton SJ, Krasel C, Bailey CP, Henderson G, Kelly E. Endomorphin-2: A biased agonist at the mu-opioid receptor. Mol Pharmacol. 2012; 82:178–188. [PubMed: 22553358]

Sayre LM, Portoghese PS. Stereospecific synthesis of the 6. alpha.-and 6. beta.- amino derivatives of naltrexone and oxymorphone. J Org Chem. 1980; 45:3366–3368.

Scheibe SD, Bennett DB, Spain JW, Roth BL, Coscia CJ. Kinetic evidence for differential agonist and antagonist binding to bovine hippocampal synaptic membrane opioid receptors. J Biol Chem. 1984; 259:13298–13303. [PubMed: 6092373]

Schulz S, Mayer D, Pfeiffer M, Stumm R, Koch T, Höllt V. Morphine induces terminal micro-opioid receptor desensitization by sustained phosphorylation of serine-375. EMBO Journal. 2004; 23:3282–3289. [PubMed: 15272312]

Spivak CE, Oz M, Beglan CL, Shrager RI. Diffusion delays and unstirred layer effects at monolayer cultures of Chinese hamster ovary cells: radioligand binding, confocal microscopy, and mathematical simulations. Cell Biochem and Biophys. 2006; 45:43–58. [PubMed: 16679563]

Swaminath G, Xiang Y, Lee TW, Steenhuis J, Parnot C, Kobilka BK. Sequential binding of agonists to the beta2 adrenoceptor. Kinetic evidence for intermediate conformational states. J Biol Chem. 2004; 279:686–691. [PubMed: 14559905]

Tan M, Groszer M, Tan AM, Pandya A, Liu X, Xie C-W. Phosphoinositide 3-kinase cascade facilitates mu-opioid desensitization in sensory neurons by altering G-protein-effector interactions. J Neurosci. 2003; 23:10292–10301. [PubMed: 14614088]

Virk MS, Williams JT. Agonist-Specific Regulation of mu-Opioid Receptor Desensitization and Recovery from Desensitization. Mol Pharmacol. 2008; 73:1301–1308. [PubMed: 18198283]

Werling LL, Puttfarcken PS, Cox BM. Multiple agonist-affinity states of opioid receptors: regulation of binding by guanyl nucleotides in guinea pig cortical, NG108-15, and 7315c cell membranes. Mol pharmacol. 1988; 33:423–431. [PubMed: 2833686]

Wüster M, Costa T. Sodium regulation of opioid agonist binding is potentiated by pertussis toxin. Biochem and Biophys Res Comm. 1984; 123:1107–1115. [PubMed: 6091647]

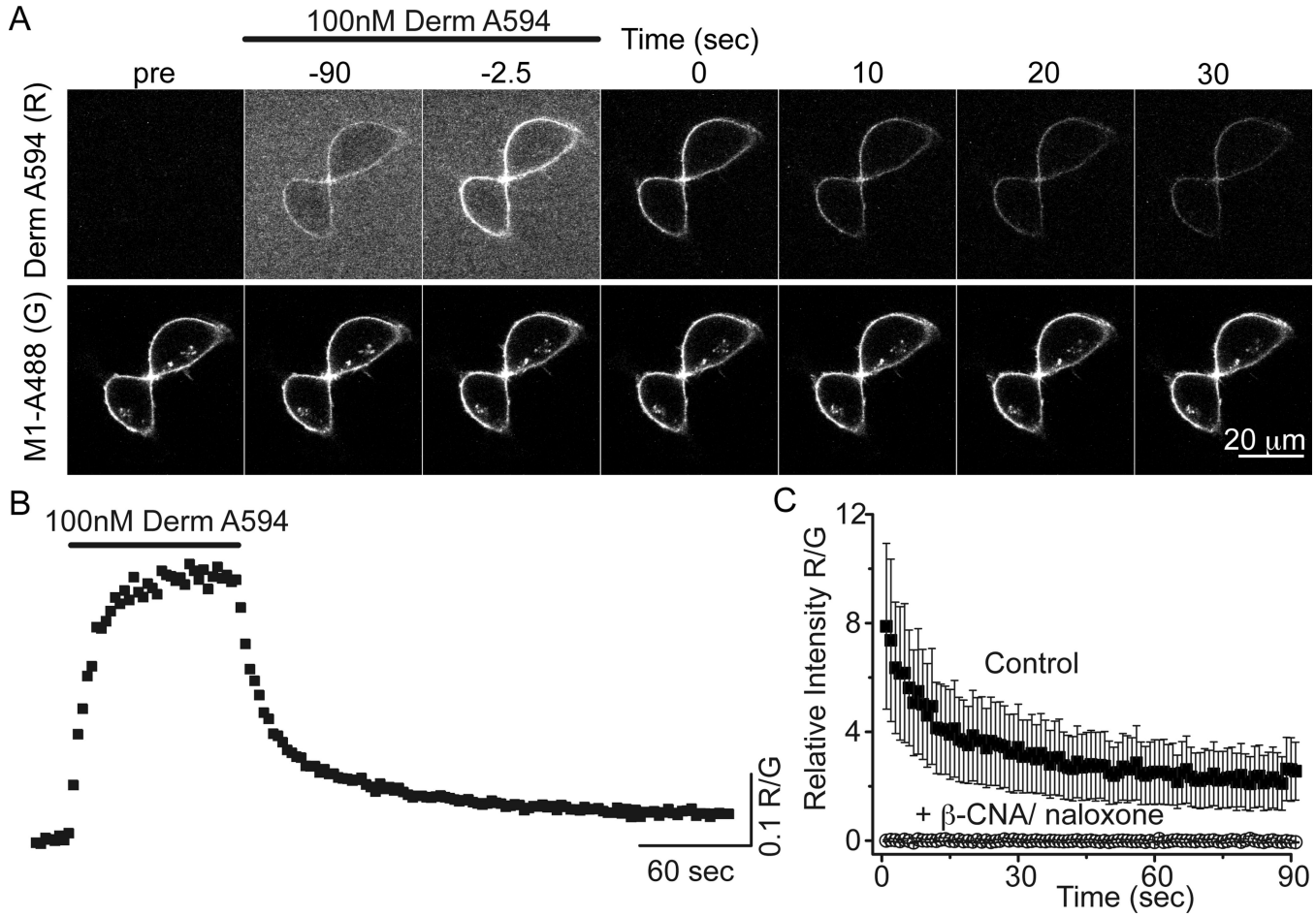

Figure 1. Imaging binding and unbinding of dermorphin A594

A, FLAG-MOR in HEK 293 cells were labeled with M1 anti FLAG antibody conjugated Alexa488 (M1 A488) to visualize receptors localized on the plasma membrane. Dermorphin Alexa 594 (100 nM, derm A594) was applied for 90 sec (wash in at t= −90 washout at t=0 in A). Derm A594 binding and unbinding were assessed by imaging M1 A488 and derm A594 every 2.5 seconds with images from selected timepoints shown. Scale: 20 µm. B, Ratiometric imaging of derm A594: M1 A488 (R/G) intensity was used to quantify binding and unbinding of agonist to receptor from the experiment shown in A. C, Specificity of binding was assessed by determining the relative fluorescence intensity (R/G) of derm A594 bound immediately after application of derm A594 (5 min, 500 nM) under control conditions or on cells pretreated with β-CNA (1 µM, 5 min) and bathed in naloxone (10 µM). Avg. ± sem. (ctrl n=5, β-CNA/naloxone n=6)

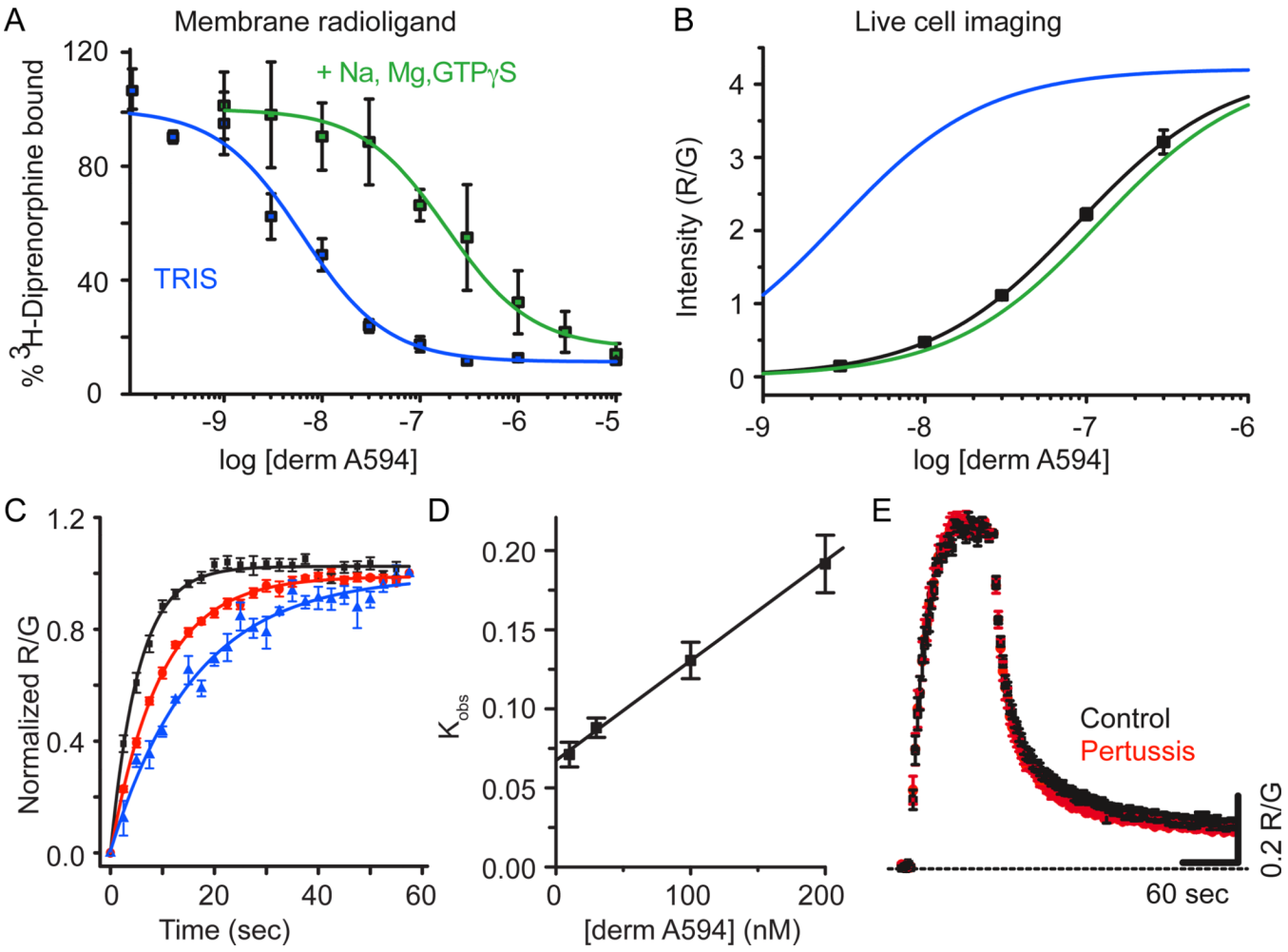

Figure 2. Derm A594 binding to FLAG-MOR in live cells is relatively low affinity

A, Steady state displacement of [^{3}H] diprenorphine (0.2 nM) with increasing concentrations of derm A594 (0 – 10 μM) from FLAG-MOR HEK 293 cell membranes was measured in TRIS alone (blue) or TRIS with Na^+, Mg^{2+}, and GTPγS (green) and fit with one site non-linear regression to define high and low affinity binding of derm A594 to FLAG-MOR. The best fit of the data are plotted. Average of 3 experiments performed in duplicate. B, Steady state binding of derm A594 in live FLAG-MOR HEK 293 cells was relatively low affinity. Cells were incubated in stated concentrations of derm A594, imaged and relative fluorescence intensity was measured. Data were fit with the Hill equation and the best fit is plotted (black), n= 5–11. High and low affinity binding curves from [^{3}H] diprenorphine competition binding experiments shown in "A" are overlaid in blue and green respectively using the K_i values from competition binding experiments and the slope and R/G_{max} values from steady state whole cell derm A594 binding to simulate expected results. C, Kinetics of derm A594 binding. Derm A594 was applied at 10 (blue), 30, 100 (red) and 200 nM (black) and the apparent association rates were determined by fitting to a single exponential decay function. For display, binding was normalized relative to the amount of derm A594 bound at the end of the 1 min period and averaged results are plotted, n= 4– 6. D, Linear fit of the apparent association rate from average data in "C" plotted as a function of derm A594 concentration. The plotted line has a slope of 612,000 mol^{-1} sec^{-1} and an intercept of 0.068 sec^{-1} giving a calculated K_d of 110 nM. E, Binding and unbinding kinetics were unaffected by pertussis toxin treatment. Cells were either untreated (black) or treated with pertussis

toxin (red) (100 ng/ml, overnight). Derm A594 (100 nM) was applied for 90 sec at the indicated time and rapidly washed. All values are averages +/− sem. (ctrl n=6, ptx n=5)

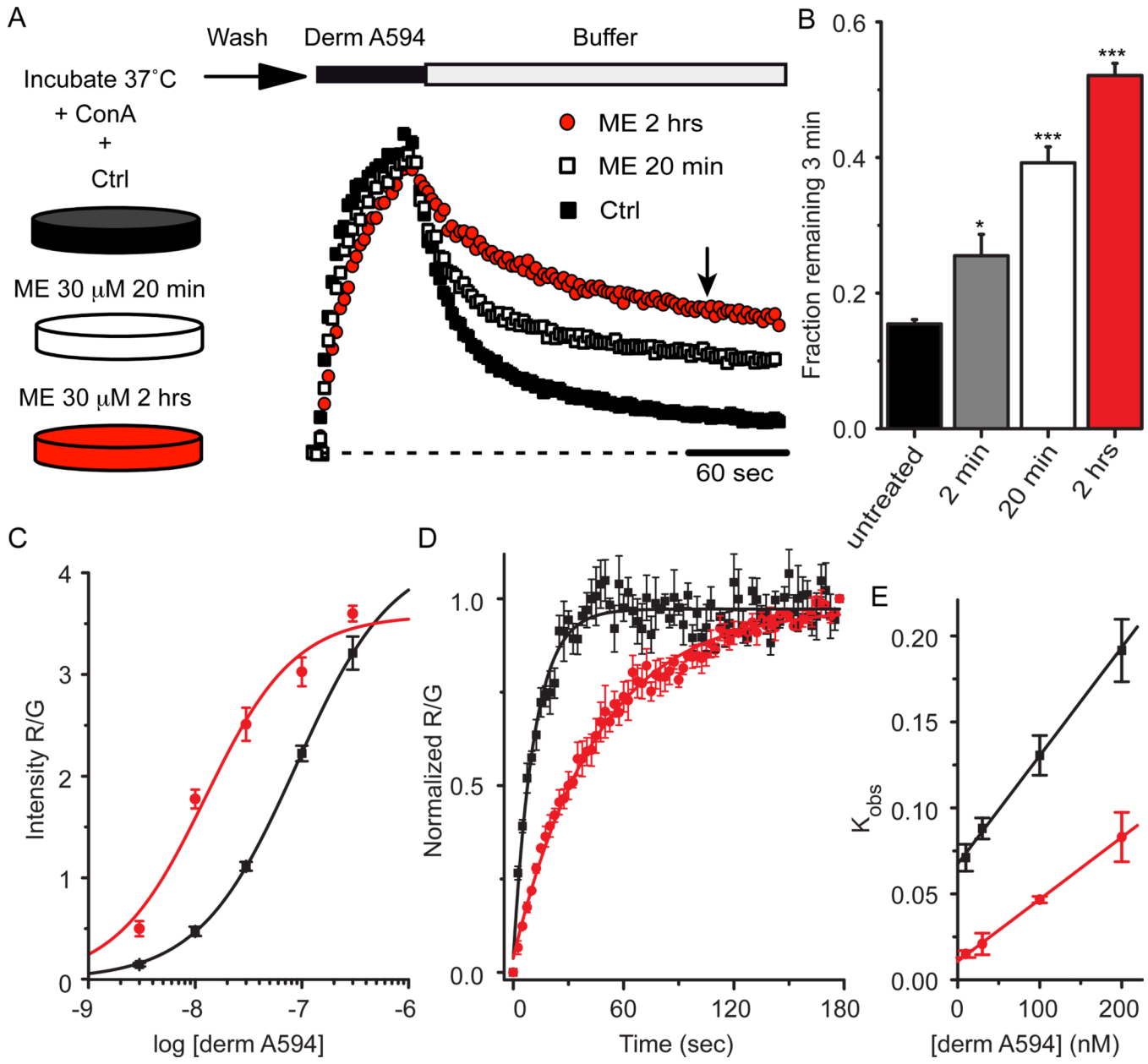

Figure 3. MOR retained a memory of previous agonist exposure

A, FLAG-MOR expressing cells were incubated either under control (black squares) conditions or in the presence of ME 30 μM for 20 min (open squares) or 2 hrs (red circles) as indicated. After washing out ME, cells were imaged while derm A594 (100 nM, 60 sec) was applied. Individual examples are shown normalized to the relative fluorescence intensity (R/G) immediately after washout of derm A594. B, Summary data quantifying the fraction of derm A594 that remained bound to the receptor 3 minutes after washout (indicated by arrow in "A") in cells that were untreated or treated with ME 30 μM for 2 min, 20 min or 2 hrs and results are shown (n=6–11, * $p< 0.05$, *** $p< 0.001$ compared to untreated, one-way ANOVA, Tukey post hoc). C, Steady state binding was carried out as described in figure 2b after pre-treatment of cells with ME for 2 hrs and was fit using the Hill equation and plotted (n=7–19 cells for each concentration). Data from untreated cells (black) shown in figure 2b and data from cells incubated with ME (red) are plotted. D,

Average observed association of derm A594 (30 nM) in untreated (black) and ME pretreated (30 μM 2 hrs, red) cells. E, Plot of average observed association rate of derm A594 after ME treatment (red) is plotted as a function of derm A594 concentration. The linear fit has a slope of 353,000 mol^{-1} sec^{-1} and an intercept of .011 sec^{-1} yielding a K_d of 32nM n=4 each. Data from untreated cells (black) shown in figure 2d are also plotted.

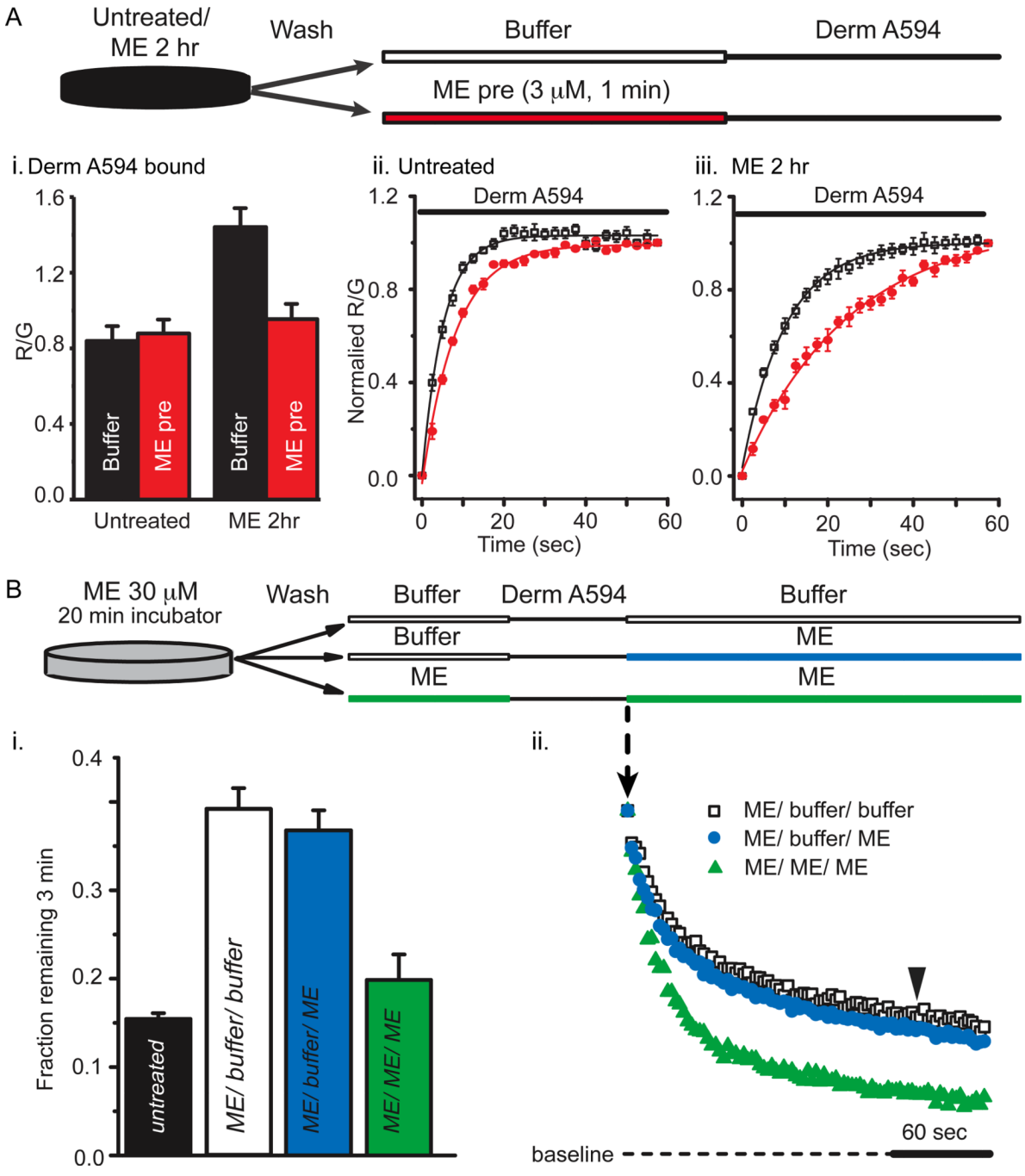

Figure 4. ME unbinds slowly after prolonged ME treatment

A, The amount of derm A594 bound relative to M1 A488 was measured in cells either untreated “ii” or treated with ME (30 μM, 2 hrs) “iii”. After treatment (untreated or ME 2 hrs), cells were washed with buffer and then subjected to a short pulse of buffer (black) or ME (3 μM, 60 sec, red) immediately preceding derm A594 application (200 nM, 60 sec) as diagrammed. A-i, Binding of derm A594 was imaged and the relative amount of derm A594 bound after 60 seconds (R/G) was measured and plotted the average normalized amount of derm A594 that bound is plotted. A-ii, iii, Binding of derm A594 (200nM) is plotted as a function of time in untreated (ii) or ME (30 μM, 2 hrs) treated cells (iii) and prepulsed with either buffer (black) or ME (3 μM, 60 sec, red) n=5–6 each. B, derm A594 (100 nM, 60 sec)

was applied to cells that had been treated with ME (30 μM, 20 min) and washed with buffer (see diagram). Unbinding of derm A594 was monitored while washing with either buffer (ME/ buffer/ buffer, open squares) or ME (3 μM, ME/ buffer/ ME, blue). ME (3 μM, 1 min) was also pulsed both immediately before and following derm A594 binding to cells that were modulated by ME (30 μM, 20 min) to determine whether residual ME had an effect on derm A594 unbinding kinetics (green, ME/ ME/ ME). Averaged data in “i” shows fraction of derm A594 remaining 3 minutes after washout (n= 7–11, indicated by arrowhead in “ii”) and individual examples of derm A594 unbinding under each condition are shown in “ii”.

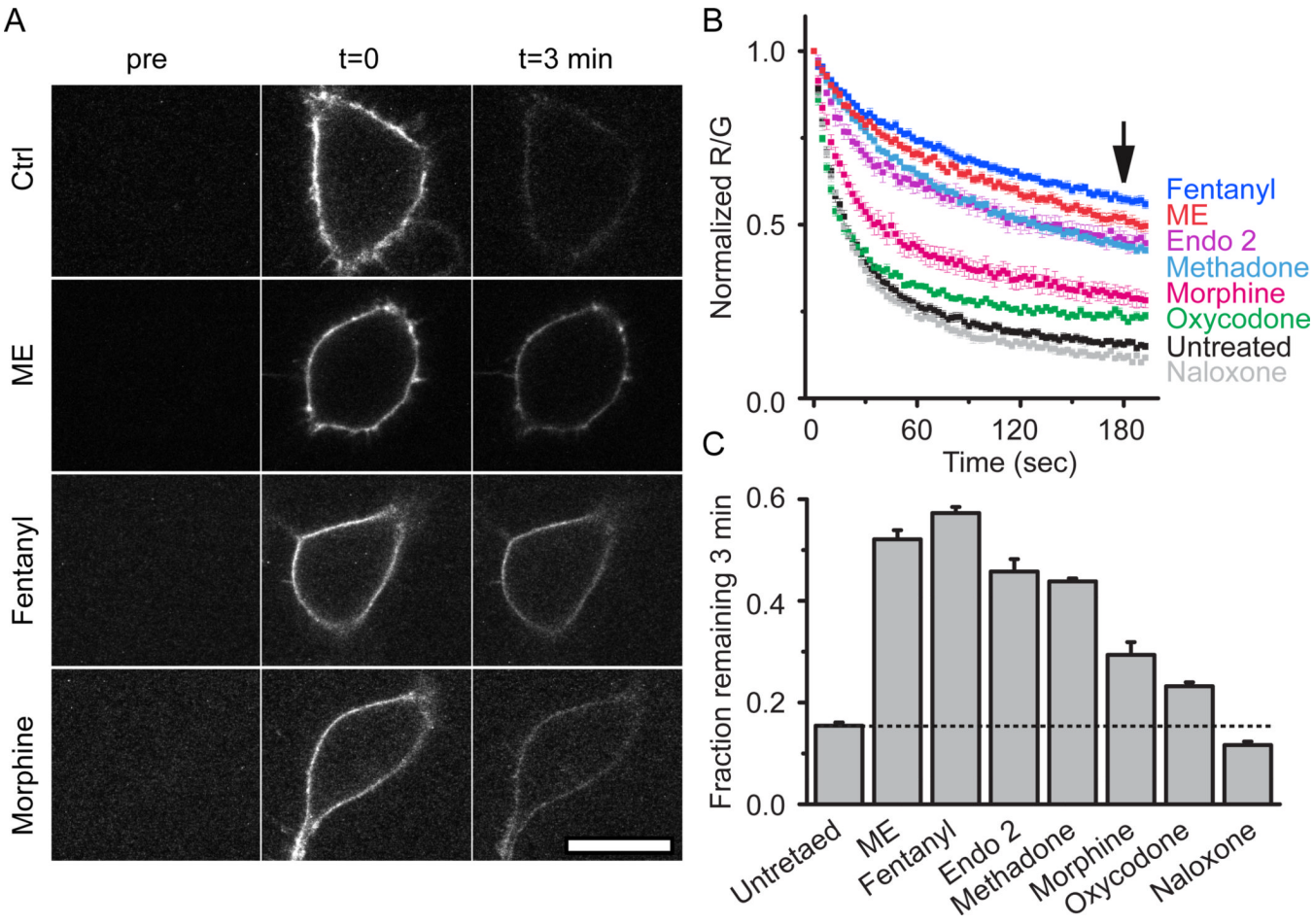

Figure 5. Ligand dependence of receptor modulation

A, Images taken either before (pre), immediately after (t=0), or 3 minutes after (t=3 min) application and rapid washout of derm A594 (100 nM, 90 sec). Images show derm A594 bound to the plasma membrane of cells expressing FLAG-MOR that were either untreated (ctrl), or treated with ME, fentanyl or morphine for 2 hrs. Scale = 20 μM. B, Quantification of unbinding of derm A594 as shown in "A" following 2 hr pre-treatment with the indicated opioid ligands. Images were taken every 2.5 sec imaging both M1 488 and derm A594. Averaged, normalized ratiometric intensity is plotted. Average±sem, n= 6–9. Arrow shows time=3 min after washout C, Fraction of derm A594 remaining at t=3 min relative to t=0 from data shown in "B" average±sem. All treatments except naloxone resulted in a significant change in the fraction bound after 3 min $P < 0.05$, ANOVA, Tukey post hoc.

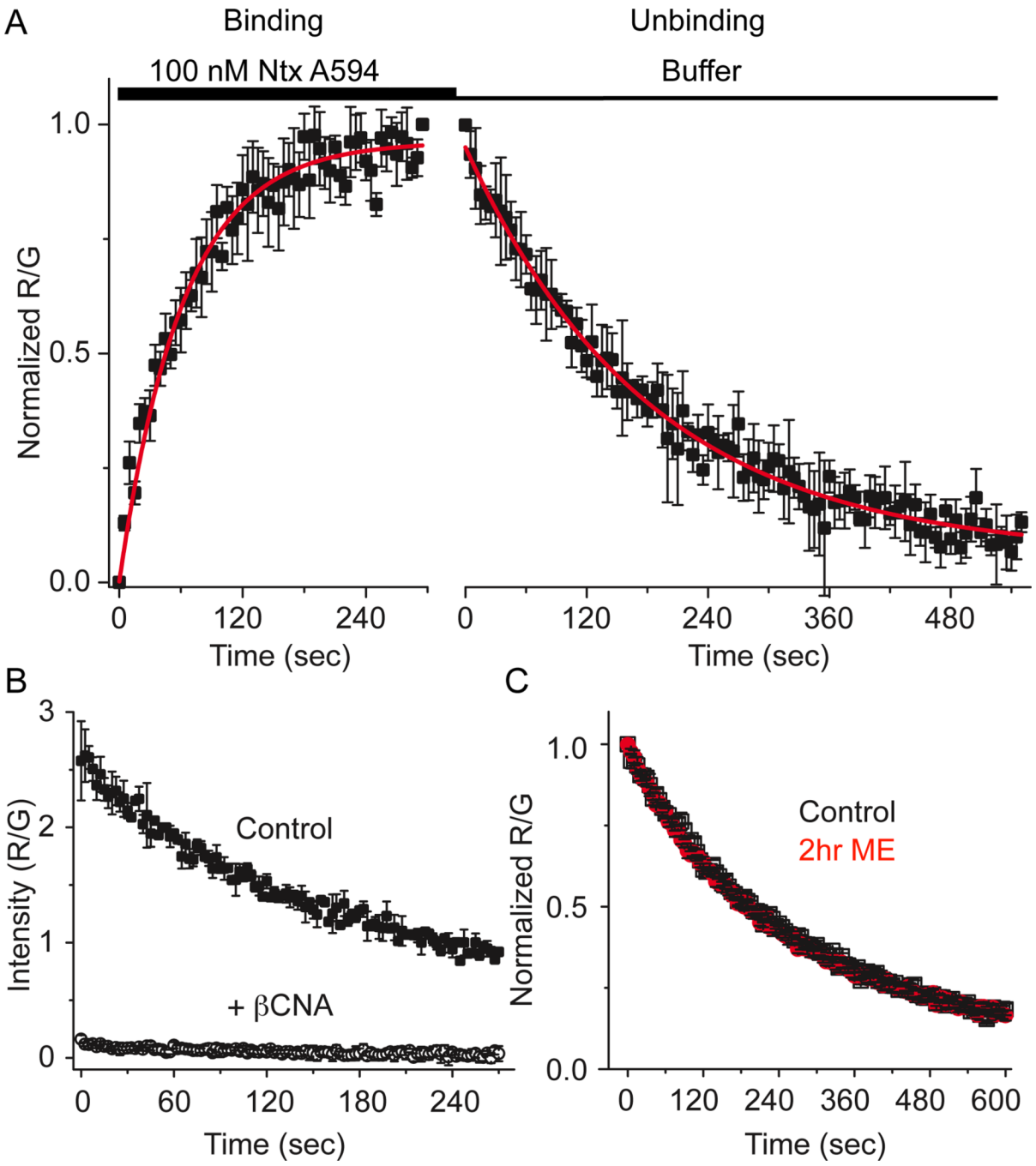

Figure 6. Unbinding of naltrexamine alexa594 was not affected by previous agonist exposure

A, Binding kinetics of the antagonist ntx A594 were measured by applying ntx A594 (100 nM, 5 min) and imaging binding and washout relative to M1–488 intensity (R/G). Binding and unbinding was plotted and fit with a single exponential decay formula (tau association= 65.8±5.5 sec, tau off =184±6.1 sec, n=4 each, average±sem). B, Preincubation of cells with the irreversible antagonist β-CNA (1 μM, 5 min) prevented all binding when measured by the fluorescence intensity immediately after washout of ntx A594 (300 nM, 90 sec) verifying the specificity of binding (n=2 ctrl, n=4 β-CNA mean±sd). C, Ntx A594 (300 nM, 90 sec) was applied and unbinding of ntx A594 was imaged from cells either untreated (black) or pre-treated with ME (30 μM, 2 hr) (red) n=5 each, average±sem.

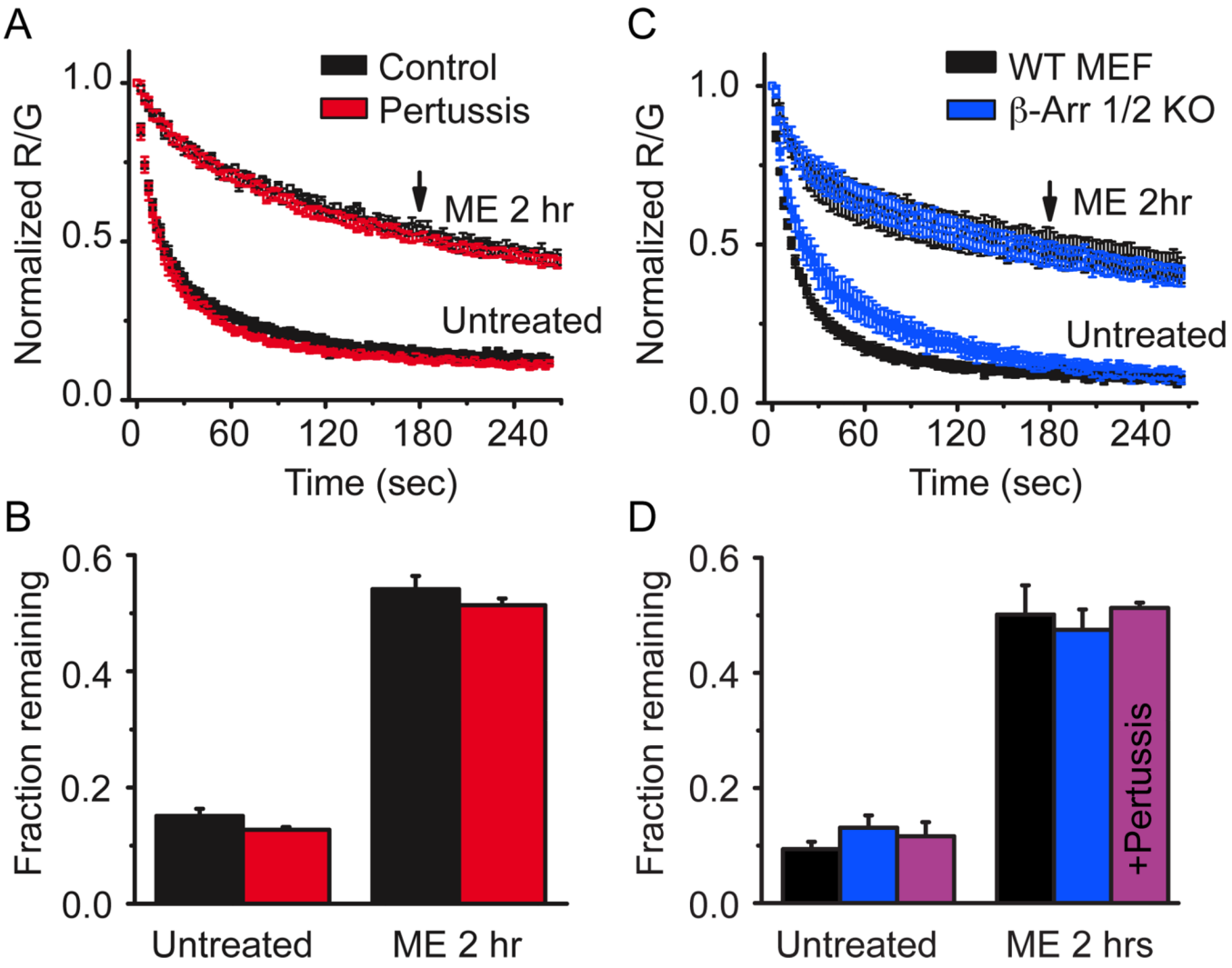

Figure 7. Modulation was independent of G-protein signaling and β-arrestins

A, FLAG-MOR expressing HEK 293 cells were either untreated (black) or treated with pertussis toxin (100 ng/ml overnight) (red) and the unbinding of derm A594 (100 nM, 90 sec) was imaged under control conditions or on cells subjected to agonist pretreatment (ME 30 μM, 2 hrs). Normalized average data are plotted n=3–6. B, The fractional amount of derm A594 that remained bound to cells 3 min after washout was quantified relative to the receptor fluorescence intensity. C, Mouse embryonic fibroblasts cultured from β-arrestin 1/2 double knockout mouse embryos (blue) or their wildtype controls (black) were either untreated or pre-treated with ME (30 μM, 2 hrs) and unbinding of derm A594 (100 nM, 90 sec) was imaged and normalized data are shown. D, Quantification of the fraction of derm A594 remaining 3 minutes after washout from WT (black) and β-arr 1/2 d.k.o. MEF cells (blue) shown in "C", n=5 each. Additionally, β-arr 1/2 d.k.o. MEF cells were treated with pertussis toxin (100 ng/ml overnight) and the fraction of derm A594 remaining in untreated and ME treated cells is shown (purple) n=4 each. All points are average± sem.

Table 1

Summary of derm A594 and Ntx A594 affinity measurements. [^{3}H] diprenorphine competition performed in crude membrane preparations in the presence and absence of Na^+, Mg^{2+}, and GTPγS (K_i ±sd, Fig 2A) revealed low and high affinity states of derm A594 binding. Kinetic affinity measurements from live cells were calculated from initial apparent binding kinetics measured for a range of derm A594 concentrations performed in live cells untreated and pretreated with ME 2 hrs (K_d ±error range Fig 2C,D). Steady state binding of derm A594 to live cells untreated and pretreated with ME 2 hrs (EC_{50} ±95% confidence interval, Fig 2B, 3B) are shown demonstrating increased affinity after ME treatment. Affinity of Ntx A594 was based on measurement of apparent on rate and off rate of ntx A594 (100nM, 5 min) (Kd± error range, Fig 6B). Ntx A594 shows similar affinity to derm A594 despite different kinetics.

Ligand	**Assay**	**Affinity (nM)**
Derm A594	Radioligand competition	2.9 +/− 0.8 (K_i)
	+Na^+, Mg^{2+}, GTPγS	120 +/− 40nM (K_i)
	Association kinetics	111 (85 – 149) (K_d)
	Association kinetics post ME 2hrs	32 (24 – 42(K_d)
	Steady state imaging	85 (50 – 142) (EC_{50})
	Steady state post ME 2hrs	11.6 (8.4 – 16.2) (EC_{50})
Ntx A594	Kinetics	53 (44 – 65) (K_d)